as described [48]. Reverse transcriptase reactions were performed with SuperScript VILO (Invitrogen), and qPCRs were performed with TAKARA SYBR Premix Ex Taq (TaKaRa), according to the manufacturer's instructions. Individual mature miRNA expression analysis was performed with the miScript system (Qiagen, Hilden, Germany) according to the manufacturer's instructions. Expression levels of mature miRNAs in the cells treated with TERT-specific siRNAs or the calibrator negative control siRNA were estimated by RT-qPCR in triplicate with the specific miScript primers (Qiagen).

4.3. shRNA Transduction, RNA Extraction and Expression Analysis by RT-qPCR

shRNAs targeting TERT and BRG1 were constructed by The RNAi Consortium, and shRNAs targeting NS were constructed in-house using the pLKO.1-puro vector. The target sequence of each shRNA was as follows [21]; sh-TERT#1 (clone ID: TRCN0000219794), 5'-CCTGCGTTTGGTGG ATGATTT-3': sh-TERT#2 (clone ID: TRCN0000179552), 5'-GACATGGAGAACAAGCTGTTT-3': sh-BRG1#1 (clone ID: TRCN0000015549), 5'-CCCGTGGACTTCAAGAAGATA-3': sh-BRG1#2 (clone ID: TRCN0000015552), 5'-CGGCAGACACTGTGATCATTT-3': sh-NS#1, 5'-GCACTGTCTG AGGAGACTACA-3': sh-NS#2, 5'-GGAGGCTCTTCTTAGGGAAGC-3'. sh-GFP was used as the control. To suppress TERT expression in HeLa cells, amphotropic lentiviruses were created with the pLKO.1-puro vectors, and the viral sup was used for infection. After infection, the cells were selected using puromycin (2 μg/mL) for three days. Total RNAs were extracted with TRIzol (Invitrogen) and a FastPure RNA kit (TaKaRa) according to the manufacture's protocols. Small RNA fractions were extracted using mirVana miRNA Isolation Kit (Ambion, Austin, TX, USA), followed by ethanol precipitation at −20 °C overnight. Reverse transcriptions were performed by using miScript Reverse Transcription Kit (Qiagen), and RT-qPCR was performed by using LightCycler 480 SYBR Green I Master (Roche Diagnostics, Mannheim, Germany), according to the manufacturer's protocol. miScript primers (Qiagen) were used for the detection of mature miRNAs. Primer pairs used for primary transcripts of miRNAs and precursor miRNAs were previously designed [49,50]. *U6* was used as the reference. All reactions were performed in triplicate.

4.4. Library Construction and Sequencing

RNAs of 15 to 50 nt in length were included in the initial screen with THP-1 cells to explore changes in a broad range of small RNA classes. For efficiency, RNAs from individual samples were labeled using barcode sequences, and six samples were pooled into one library to be sequenced together in one lane of the Illumina Genome Analyzer (Illumina, San Diego, CA, USA) for the large-scale screening of RNA populations. The procedures for the short RNA library constructions were essentially as described in [51]. The library for the deep sequencing of miRNAs was constructed using the Small RNA Sample Kit (Illumina), according to the manufacturer's instructions. Libraries were sequenced using the Genome Analyzer (Illumina).

RNA fractionation was performed as described previously [24]. Cell lysis homogenization and extraction of total RNA were performed with TRIzol (Invitrogen), according to the manufacturer's instructions. Then FastPure RNA kit (TaKaRa) was used for RNA purification and fractionation, according to modified manufacturer's instructions. After phase separation of TRIzol, the aqueous phase was mixed with the same amount of 70% ethanol and flowed through a filter cartridge to capture

RNA longer than 200 nt. The flow through was then mixed with ethanol to obtain a 50% final concentration and flowed through a new filter cartridge to capture RNAs smaller than 200 nt. After RNA binding to the filter cartridge, each bound RNA was washed three times with 700 μL of treble ethanol diluted wash buffer and eluted with elution buffer.

Three micrograms of the short RNA fraction were used for each library construction after denaturation at 65 °C for 5 min. For a capped library, the phosphatase reaction and decapping reaction were done before sequence linker ligation. The phosphatase reaction was performed at 37 °C for 2 h in 30 μL reaction volume with 30 units of Antarctic phosphatase (NEB, Ipswich, MA, USA), according to the manufacturer's instructions. Tobacco acid pyrophosphatase reaction for removing the CAP structure was performed at 37 °C for 1 h with 6 units of tobacco acid pyrophosphatase (EPICENTRE, Madison, WI, USA), according to the manufacturer's instructions. For a hydroxylated library, the phosphorylation reaction was done before linker ligation. The T4 polynucleotide kinase reaction for phosphorylation was performed at 37 °C for 30 min in 100 μL reaction volume with 40 units of T4 polynucleotide kinase (NEB), according to the manufacturer's instructions. After each enzyme reaction, products were purified by phenol:chloroform:isoamyl alcohol (25:24:1) extraction and ethanol precipitation.

After pretreatment, each short RNA was ligated with a PAGE purified RNA-DNA hybrid 5' adaptor tag containing a sample-specific four-nucleotide tag sequence (5'-ACAGGTTCAGAGTT CTACAGXXXXA-OH-3') and 3' adaptor mix containing 3' biotinylation and 5' phosphorylation (5'-phosphate-uuuTCGTATGCCGTCTTCTGCTTG-Biotin-3') with T4 RNA ligase (TaKaRa) for 16 h at 15 °C. Tag-ligated short RNAs were purified with PAGE extraction, and an RT-PCR reaction was performed for cDNA synthesis with reverse transcriptase and primer L1 (5'-CAAGCAGA AGACGGCATACGA-3'). The subsequent PCR reaction was performed with the same primer L1 and primer U3 (5'-ACAGGTTCAGAGTTCTACAG-3'). RT products were calibrated to determine the ratio of products derived from individual knockdown and pretreated samples in the library and purified by PAGE extraction.

cDNA derived from RT-PCR was amplified by PCR to add sequencing of the oligonucleotide sequence with primer L1 and primer U1 (5'-AATGATACGGCGACCACGACAGGTTCAGAGT TCTACAG-3') and purified with PAGE extraction.

Purified PCR products for sequencing were sequenced using Genome Analyzer (Illumina) with the sequencing primer (5'-CGGCGACCACGACAGGTTCAGAGTTCTACAG-3'), according to the manufacturer's instructions.

4.5. Bioinformatics

In total, 61.4 million sequences were obtained in the initial screening experiment and an additional 23.6 million in the experiment focused on the miRNA fraction. We applied the program TagDust [52] to the sequenced libraries to remove all captured siRNA and adaptor sequences used in the experiment. Furthermore, we removed all sequences that were found less than 10 times in all experiments. All obtained reads were mapped to the human genome (hg19) using Delve. In brief, Delve uses a pair hidden Markov model (pHMM) to iteratively map reads to the genome and to estimate position-dependent error probabilities. After all error probabilities are estimated, individual reads are

placed into a single position on the genome, where the alignment has the highest probability of being true according to the pHMM model. Phred-scaled mapping qualities, reflecting the likelihood of the alignment at a genome position, are also reported. Reads mapping with a quality of less than 10 (<90% chance of true) were discarded.

To assign reads to individual miRNA loci, we intersected mapping locations with the genomic boundaries of known miRNAs obtained from GENCODE (http://www.gencodegenes.org/) using BEDtools [53]. We used the same approach with additional annotation categories to obtain a global pre-library overview of what was sequenced (Figures S2–S4, S6 and S7).

To detect differentially expressed reads in our libraries, we first summed the number of reads mapping to each miRNA and applied the R package edgeR [54]. We used the exact test to detect differences in read counts exactly as described in the documentation using the short RNA example. In the absence of replicas, we estimated the read dispersion by treating both the control and test libraries as replicas. Differentially-expressed miRNAs with a false discovery rate less than 5% alongside their concentration and fold-changes are listed in Tables S2–S4 for all comparisons.

In Figure S5a, the sequences were analyzed with TagDust and mapped to the human genome (hg18) using the program, Nexalign [55].

4.6. Purification of TERT Complexes and Isolation of RNAs

Purification of TERT complexes was performed as described previously [19]. For this, 2×10^8 HeLa-S3 cells expressing or lacking (control) TAP-TERT were lysed in 5 mL of Lysis Buffer A (LBA; 20 mM Tris-HCl pH 7.4, 150 mM NaCl, 0.5% NP-40, 0.1 mM DTT) and incubated for 30 min on ice. The lysate was then centrifuged at 16,000× *g* for 20 min at 4 °C. The supernatant was incubated with the anti-FLAG (M2) antibody conjugated agarose (SIGMA, Saint Louis, MO, USA) overnight at 4 °C. The beads were washed 3 times with LBA and eluted with 3× FLAG peptide (150 ng/μL). The resulting elution was incubated with protein A agarose beads (PIERCE, Rockford, IL, USA) and an anti-HA antibody (F7; Santa Cruz, Santa Cruz, CA, USA) for 4 h at 4 °C. The beads were washed 3 times with LBA, and RNA was isolated using TRIzol (Invitrogen). RNA samples prepared in this manner were analyzed with an Experion capillary electrophoresis device (Bio-Rad, Hercules, CA, USA) to visualize RNA species. Twenty percent of the RNA was used for RT-qPCR, and the remaining 80% was analyzed by deep sequencing. RT-qPCR was performed with a LightCycler 480 II (Roche Diagnostics), according to the manufacturer's protocols. The TaqMan Gene Expression Assay system was used for human *TERC* analysis. The expression levels of *RMRP* were detected using the following primers and probe [19]; forward primer (5'-GAGAGTGCCACGTGC ATACG-3'), reverse primer (5'-CTCAGCGGGATACGCTTCTT-3'), VIC-labeled TaqMan MGB probe (5'-ACGTAGACATTCCCC-3').

5. Conclusions

Our comprehensive analysis clearly demonstrated TERT-based positive regulation of miRNAs in human cells. Involvement of BRG1 and NS, as well as TERT in the regulation indicates that the TBN complex, and not the telomerase complex, may be in charge of this novel function of TERT. It is now speculated that TERT plays multiple roles in both physiological and pathological processes, not only

by affecting telomere homeostasis, but also by regulating small RNA homeostasis, including both endogenous siRNA and miRNA. The detailed mechanisms of TERT-mediated miRNA regulation will be uncovered in future studies.

Supplementary Materials

Supplementary materials can be found at http://www.mdpi.com/1422-0067/16/01/1192/s1.

Acknowledgments

This work was supported in part by a Grant-in-Aid for Young Scientists (A) 21689012 (Kenkichi Masutomi) and a Grant-in-Aid for Young Scientists (B) 21791579 (Yoshiko Maida) from the Ministry of Education, Culture, Sports, Science and Technology; a research grant for the RIKEN Omics Science Center from MEXT (Yoshihide Hayashizaki); The Mitsubishi Foundation (Kenkichi Masutomi); and the Grant of the Princess Takamatsu Cancer Research Fund 13-24520 (Yoshiko Maida).

Author Contributions

Kenkichi Masutomi, Yoshihide Hayashizaki, Timo Lassmann, Yoshiko Maida, Yasuhiro Tomaru, Piero Carninci and Yoshinari Ando conceived of and designed the experiments. Yoshiko Maida, Yasuhiro Tomaru, Mami Yasukawa, Yoshinari Ando, Miki Kojima, Vivi Kasim, Christophe Simon and Carsten O. Daub performed the experiments. Timo Lassmann and Piero Carninci analyzed the data. Timo Lassmann, Yoshiko Maida and Yasuhiro Tomaru wrote the paper.

Conflicts of Interest

The authors declare no conflict of interest.

References

1. Bartel, D.P. MicroRNAs: Genomics, biogenesis, mechanism, and function. *Cell* **2004**, *116*, 281–297.
2. Siomi, H.; Siomi, M.C. Posttranscriptional regulation of microRNA biogenesis in animals. *Mol. Cell* **2010**, *38*, 323–332.
3. O'Donnell, K.A.; Wentzel, E.A.; Zeller, K.I.; Dang, C.V.; Mendell, J.T. c-Myc-regulated microRNAs modulate E2F1 expression. *Nature* **2005**, *435*, 839–843.
4. Loffler, D.; Brocke-Heidrich, K.; Pfeifer, G.; Stocsits, C.; Hackermuller, J.; Kretzschmar, A.K.; Burger, R.; Gramatzki, M.; Blumert, C.; Bauer, K.; *et al.* Interleukin-6 dependent survival of multiple myeloma cells involves the Stat3-mediated induction of microRNA-21 through a highly conserved enhancer. *Blood* **2007**, *110*, 1330–1333.
5. Brock, M.; Trenkmann, M.; Gay, R.E.; Michel, B.A.; Gay, S.; Fischler, M.; Ulrich, S.; Speich, R.; Huber, L.C. Interleukin-6 modulates the expression of the bone morphogenic protein receptor type II through a novel STAT3-microRNA cluster 17/92 pathway. *Circ. Res.* **2009**, *104*, 1184–1191.
6. Iliopoulos, D.; Jaeger, S.A.; Hirsch, H.A.; Bulyk, M.L.; Struhl, K. STAT3 activation of miR-21 and miR-181b-1 via PTEN and CYLD are part of the epigenetic switch linking inflammation to cancer. *Mol. Cell* **2010**, *39*, 493–506.

7. Ma, L.; Teruya-Feldstein, J.; Weinberg, R.A. Tumour invasion and metastasis initiated by microRNA-10b in breast cancer. *Nature* **2007**, *449*, 682–688.
8. Lee, Y.B.; Bantounas, I.; Lee, D.Y.; Phylactou, L.; Caldwell, M.A.; Uney, J.B. Twist-1 regulates the miR-199a/214 cluster during development. *Nucleic Acids Res.* **2009**, *37*, 123–128.
9. Taganov, K.D.; Boldin, M.P.; Chang, K.J.; Baltimore, D. NF-κB-dependent induction of microRNA miR-146, an inhibitor targeted to signaling proteins of innate immune responses. *Proc. Natl. Acad. Sci. USA* **2006**, *103*, 12481–12486.
10. Baer, C.; Claus, R.; Plass, C. Genome-wide epigenetic regulation of miRNAs in cancer. *Cancer Res.* **2013**, *73*, 473–477.
11. Weinrich, S.L.; Pruzan, R.; Ma, L.; Ouellette, M.; Tesmer, V.M.; Holt, S.E.; Bodnar, A.G.; Lichtsteiner, S.; Kim, N.W.; Trager, J.B.; *et al.* Reconstitution of human telomerase with the template RNA component hTR and the catalytic protein subunit hTRT. *Nat. Genet.* **1997**, *17*, 498–502.
12. Gonzalez-Suarez, E.; Samper, E.; Ramirez, A.; Flores, J.M.; Martin-Caballero, J.; Jorcano, J.L.; Blasco, M.A. Increased epidermal tumors and increased skin wound healing in transgenic mice overexpressing the catalytic subunit of telomerase, mTERT, in basal keratinocytes. *EMBO J.* **2001**, *20*, 2619–2630.
13. Artandi, S.E.; Alson, S.; Tietze, M.K.; Sharpless, N.E.; Ye, S.; Greenberg, R.A.; Castrillon, D.H.; Horner, J.W.; Weiler, S.R.; Carrasco, R.D. *et al.* Constitutive telomerase expression promotes mammary carcinomas in aging mice. *Proc. Natl. Acad. Sci. USA* **2002**, *99*, 8191–8196.
14. Masutomi, K.; Possemato, R.; Wong, J.M.; Currier, J.L.; Tothova, Z.; Manola, J.B.; Ganesan, S.; Lansdorp, P.M.; Collins, K.; Hahn, W.C. The telomerase reverse transcriptase regulates chromatin state and DNA damage responses. *Proc. Natl. Acad. Sci. USA* **2005**, *102*, 8222–8227.
15. Sarin, K.Y.; Cheung, P.; Gilison, D.; Lee, E.; Tennen, R.I.; Wang, E.; Artandi, M.K.; Oro, A.E.; Artandi, S.E. Conditional telomerase induction causes proliferation of hair follicle stem cells. *Nature* **2005**, *436*, 1048–1052.
16. Lee, J.; Sung, Y.H.; Cheong, C.; Choi, Y.S.; Jeon, H.K.; Sun, W.; Hahn, W.C.; Ishikawa, F.; Lee, H.W. TERT promotes cellular and organismal survival independently of telomerase activity. *Oncogene* **2008**, *27*, 3754–3760.
17. Low, K.C.; Tergaonkar, V. Telomerase: Central regulator of all of the hallmarks of cancer. *Trends. Biochem. Sci.* **2013**, *38*, 426–434.
18. Li, Y.; Tergaonkar, V. Noncanonical functions of telomerase: Implications in telomerase-targeted cancer therapies. *Cancer Res.* **2014**, *74*, 1639–1644.
19. Maida, Y.; Yasukawa, M.; Furuuchi, M.; Lassmann, T.; Possemato, R.; Okamoto, N.; Kasim, V.; Hayashizaki, Y.; Hahn, W.C.; Masutomi, K. An RNA-dependent RNA polymerase formed by TERT and the RMRP RNA. *Nature* **2009**, *461*, 230–235.
20. Maida, Y.; Yasukawa, M.; Okamoto, N.; Ohka, S.; Kinoshita, K.; Totoki, Y.; Ito, T.K.; Minamino, T.; Nakamura, H.; Yamaguchi, S.; *et al.* Involvement of telomerase reverse transcriptase in heterochromatin maintenance. *Mol. Cell Biol.* **2014**, *34*, 1576–1593.
21. Okamoto, N.; Yasukawa, M.; Nguyen, C.; Kasim, V.; Maida, Y.; Possemato, R.; Shibata, T.; Ligon, K.L.; Fukami, K.; Hahn, W.C. *et al.* Maintenance of tumor initiating cells of defined genetic composition by nucleostemin. *Proc. Natl. Acad. Sci. USA* **2011**, *108*, 20388–20393.

22. Kawaji, H.; Nakamura, M.; Takahashi, Y.; Sandelin, A.; Katayama, S.; Fukuda, S.; Daub, C.O.; Kai, C.; Kawai, J.; Yasuda, J.; *et al.* Hidden layers of human small RNAs. *BMC Genomics* **2008**, *9*, doi:10.1186/1471-2164-9-157.
23. Hannon, G.J.; Maroney, P.A.; Branch, A.; Benenfield, B.J.; Robertson, H.D.; Nilsen, T.W. Accurate processing of human pre-rRNA *in vitro*. *Mol. Cell Biol.* **1989**, *9*, 4422–4431.
24. Burroughs, A.M.; Ando, Y.; de Hoon, M.J.; Tomaru, Y.; Nishibu, T.; Ukekawa, R.; Funakoshi, T.; Kurokawa, T.; Suzuki, H.; Hayashizaki, Y.; *et al.* A comprehensive survey of 3' animal miRNA modification events and a possible role for 3' adenylation in modulating miRNA targeting effectiveness. *Genome Res.* **2010**, *20*, 1398–1410.
25. Park, J.I.; Venteicher, A.S.; Hong, J.Y.; Choi, J.; Jun, S.; Shkreli, M.; Chang, W.; Meng, Z.; Cheung, P.; Ji, H.; *et al.* Telomerase modulates Wnt signalling by association with target gene chromatin. *Nature* **2009**, *460*, 66–72.
26. Cai, X.; Hagedorn, C.H.; Cullen, B.R. Human microRNAs are processed from capped, polyadenylated transcripts that can also function as mRNAs. *RNA* **2004**, *10*, 1957–1966.
27. Lee, Y.; Kim, M.; Han, J.; Yeom, K.H.; Lee, S.; Baek, S.H.; Kim, V.N. MicroRNA genes are transcribed by RNA polymerase II. *EMBO J.* **2004**, *23*, 4051–4060.
28. Borchert, G.M.; Lanier, W.; Davidson, B.L. RNA polymerase III transcribes human microRNAs. *Nat. Struct. Mol. Biol.* **2006**, *13*, 1097–1101.
29. Morlando, M.; Ballarino, M.; Gromak, N.; Pagano, F.; Bozzoni, I.; Proudfoot, N.J. Primary microRNA transcripts are processed co-transcriptionally. *Nat. Struct. Mol. Biol.* **2008**, *15*, 902–909.
30. Fujita, S.; Iba, H. Putative promoter regions of miRNA genes involved in evolutionarily conserved regulatory systems among vertebrates. *Bioinformatics* **2008**, *24*, 303–308.
31. Marson, A.; Levine, S.S.; Cole, M.F.; Frampton, G.M.; Brambrink, T.; Johnstone, S.; Guenther, M.G.; Johnston, W.K.; Wernig, M.; Newman, J.; *et al.* Connecting microRNA genes to the core transcriptional regulatory circuitry of embryonic stem cells. *Cell* **2008**, *134*, 521–533.
32. Ozsolak, F.; Poling, L.L.; Wang, Z.; Liu, H.; Liu, X.S.; Roeder, R.G.; Zhang, X.; Song, J.S.; Fisher, D.E. Chromatin structure analyses identify miRNA promoters. *Genes Dev.* **2008**, *22*, 3172–3183.
33. Corcoran, D.L.; Pandit, K.V.; Gordon, B.; Bhattacharjee, A.; Kaminski, N.; Benos, P.V. Features of mammalian microRNA promoters emerge from polymerase II chromatin immunoprecipitation data. *PLoS One* **2009**, *4*, e5279.
34. Carninci, P.; Sandelin, A.; Lenhard, B.; Katayama, S.; Shimokawa, K.; Ponjavic, J.; Semple, C.A.; Taylor, M.S.; Engstrom, P.G.; Frith, M.C.; *et al.* Genome-wide analysis of mammalian promoter architecture and evolution. *Nat. Genet.* **2006**, *38*, 626–635.
35. Dews, M.; Homayouni, A.; Yu, D.; Murphy, D.; Sevignani, C.; Wentzel, E.; Furth, E.E.; Lee, W.M.; Enders, G.H.; Mendell, J.T.; *et al.* Augmentation of tumor angiogenesis by a Myc-activated microRNA cluster. *Nat. Genet.* **2006**, *38*, 1060–1065.
36. Lin, C.H.; Jackson, A.L.; Guo, J.; Linsley, P.S.; Eisenman, R.N. Myc-regulated microRNAs attenuate embryonic stem cell differentiation. *EMBO J.* **2009**, *28*, 3157–3170.
37. Kim, J.W.; Mori, S.; Nevins, J.R. Myc-induced microRNAs integrate Myc-mediated cell proliferation and cell fate. *Cancer Res.* **2010**, *70*, 4820–4828.

38. Mestdagh, P.; Fredlund, E.; Pattyn, F.; Schulte, J.H.; Muth, D.; Vermeulen, J.; Kumps, C.; Schlierf, S.; de Preter, K.; van Roy, N.; *et al.* MYCN/c-MYC-induced microRNAs repress coding gene networks associated with poor outcome in MYCN/c-MYC-activated tumors. *Oncogene* **2010**, *29*, 1394–1404.
39. Smith, K.N.; Singh, A.M.; Dalton, S. Myc represses primitive endoderm differentiation in pluripotent stem cells. *Cell Stem Cell* **2010**, *7*, 343–354.
40. Card, D.A.; Hebbar, P.B.; Li, L.; Trotter, K.W.; Komatsu, Y.; Mishina, Y.; Archer, T.K. Oct4/Sox2-regulated miR-302 targets cyclin D1 in human embryonic stem cells. *Mol. Cell Biol.* **2008**, *28*, 6426–6438.
41. Liu, H.; Deng, S.; Zhao, Z.; Zhang, H.; Xiao, J.; Song, W.; Gao, F.; Guan, Y. Oct4 regulates the miR-302 cluster in P19 mouse embryonic carcinoma cells. *Mol. Biol. Rep.* **2011**, *38*, 2155–2160.
42. Fujita, S.; Ito, T.; Mizutani, T.; Minoguchi, S.; Yamamichi, N.; Sakurai, K.; Iba, H. miR-21 Gene expression triggered by AP-1 is sustained through a double-negative feedback mechanism. *J. Mol. Biol.* **2008**, *378*, 492–504.
43. Mallappa, C.; Nasipak, B.T.; Etheridge, L.; Androphy, E.J.; Jones, S.N.; Sagerstrom, C.G.; Ohkawa, Y.; Imbalzano, A.N. Myogenic microRNA expression requires ATP-dependent chromatin remodeling enzyme function. *Mol. Cell Biol.* **2010**, *30*, 3176–3186.
44. He, T.C.; Sparks, A.B.; Rago, C.; Hermeking, H.; Zawel, L.; da Costa, L.T.; Morin, P.J.; Vogelstein, B.; Kinzler, K.W. Identification of c-MYC as a target of the APC pathway. *Science* **1998**, *281*, 1509–1512.
45. Van de Wetering, M.; Sancho, E.; Verweij, C.; de Lau, W.; Oving, I.; Hurlstone, A.; van der Horn, K.; Batlle, E.; Coudreuse, D.; Haramis, A.P.; *et al.* The β-catenin/TCF-4 complex imposes a crypt progenitor phenotype on colorectal cancer cells. *Cell* **2002**, *111*, 241–250.
46. Ghosh, A.; Saginc, G.; Leow, S.C.; Khattar, E.; Shin, E.M.; Yan, T.D.; Wong, M.; Zhang, Z.; Li, G.; Sung, W.K.; *et al.* Telomerase directly regulates NF-κB-dependent transcription. *Nat. Cell Biol.* **2012**, *14*, 1270–1281.
47. Drevytska, T.I.; Nagibin, V.S.; Gurianova, V.L.; Kedlyan, V.R.; Moibenko, A.A.; Dosenko, V.E. Silencing of TERT decreases levels of miR-1, miR-21, miR-29a and miR-208a in cardiomyocytes. *Cell Biochem. Funct.* **2014**, *32*, 565–570.
48. Tomaru, Y.; Nakanishi, M.; Miura, H.; Kimura, Y.; Ohkawa, H.; Ohta, Y.; Hayashizaki, Y.; Suzuki, M. Identification of an inter-transcription factor regulatory network in human hepatoma cells by Matrix RNAi. *Nucleic Acids Res.* **2009**, *37*, 1049–1060.
49. Jiang, J.; Lee, E.J.; Gusev, Y.; Schmittgen, T.D. Real-time expression profiling of microRNA precursors in human cancer cell lines. *Nucleic Acids Res.* **2005**, *33*, 5394–5403.
50. Suzuki, H.I.; Yamagata, K.; Sugimoto, K.; Iwamoto, T.; Kato, S.; Miyazono, K. Modulation of microRNA processing by p53. *Nature* **2009**, *460*, 529–533.
51. Taft, R.J.; Glazov, E.A.; Cloonan, N.; Simons, C.; Stephen, S.; Faulkner, G.J.; Lassmann, T.; Forrest, A.R.; Grimmond, S.M.; Schroder, K.; *et al.* Tiny RNAs associated with transcription start sites in animals. *Nat. Genet.* **2009**, *41*, 572–578.
52. Lassmann, T.; Hayashizaki, Y.; Daub, C.O. TagDust—A program to eliminate artifacts from next generation sequencing data. *Bioinformatics* **2009**, *25*, 2839–2840.

53. Quinlan, A.R.; Hall, I.M. BEDTools: A flexible suite of utilities for comparing genomic features. *Bioinformatics* **2010**, *26*, 841–842.
54. Robinson, M.D.; McCarthy, D.J.; Smyth, G.K. edgeR: A Bioconductor package for differential expression analysis of digital gene expression data. *Bioinformatics* **2010**, *26*, 139–140.
55. Lassmann, T. Nexalign. Available online: http://134.160.84.27/osc/english/dataresource/index.html (accessed on 2009).

OPEN ACCESS Freely available online

PLOS | ONE

Eribulin Mesylate Targets Human Telomerase Reverse Transcriptase in Ovarian Cancer Cells

Satoko Yamaguchi[1], Yoshiko Maida[1], Mami Yasukawa[1], Tomoyasu Kato[2], Masayuki Yoshida[3], Kenkichi Masutomi[1]*

1 Division of Cancer Stem Cell, National Cancer Center Research Institute, Tokyo, Japan, **2** Department of Gynecology, National Cancer Center Hospital, Tokyo, Japan, **3** Department of Pathology and Clinical Laboratories, National Cancer Center Hospital, Tokyo, Japan

Abstract

Treatment of advanced ovarian cancer involves platinum-based chemotherapy. However, chemoresistance is a major obstacle. Cancer stem cells (CSCs) are thought to be one of the causes of chemoresistance, but the underlying mechanism remains elusive. Recently, human telomerase reverse transcriptase (hTERT) has been reported to promote CSC-like traits. In this study, we found that a mitotic inhibitor, eribulin mesylate (eribulin), effectively inhibited growth of platinum-resistant ovarian cancer cell lines. Eribulin-sensitive cells showed a higher efficiency for sphere formation, suggesting that these cells possess an enhanced CSC-like phenotype. Moreover, these cells expressed a higher level of hTERT, and suppression of hTERT expression by siRNA resulted in decreased sensitivity to eribulin, suggesting that hTERT may be a target for eribulin. Indeed, we found that eribulin directly inhibited RNA-dependent RNA polymerase (RdRP) activity, but not telomerase activity of hTERT *in vitro*. We propose that eribulin targets the RdRP activity of hTERT and may be an effective therapeutic option for CSCs. Furthermore, hTERT may be a useful biomarker to predict clinical responses to eribulin.

Citation: Yamaguchi S, Maida Y, Yasukawa M, Kato T, Yoshida M, et al. (2014) Eribulin Mesylate Targets Human Telomerase Reverse Transcriptase in Ovarian Cancer Cells. PLoS ONE 9(11): e112438. doi:10.1371/journal.pone.0112438

Editor: Taro Yamashita, Kanazawa University, Japan

Received August 19, 2014; **Accepted** October 6, 2014; **Published** November 6, 2014

Data Availability: The authors confirm that all data underlying the findings are fully available without restriction. All relevant data are within the paper and its Supporting Information files.

Funding: This work was supported by Grant in Aid for Scientific Research (26462544) (to SY) from Japan Society for the Promotion of Science (http://www.jsps.go.jp/english/e-grants/), Funding program for the Next Generation World-Leading Researchers (NEXT program) (to KM) from Japan Society for the Promotion of Science (http://www.jsps.go.jp/english/e-jisedai/), the Mitsubishi Foundation (to KM) (http://www.mitsubishi-zaidan.jp/en/), the Uehara Memorial Foundation (to KM) (http://www.ueharazaidan.or.jp/), and National Cancer Center Research and Development Funds (26-A-5) (to KM) (http://www.ncc.go.jp/jp/about/rinri/kaihatsu/). The funders had no role in study design, data collection and analysis, decision to publish, or preparation of the manuscript.

Competing Interests: The authors have declared that no competing interests exist.

* Email: kmasutom@ncc.go.jp

Introduction

Ovarian cancer is the most lethal of all gynecological malignancies, claiming around 150,000 lives annually worldwide. The majority of ovarian cancers are diagnosed at an advanced stage, and platinum-based chemotherapy is the standard first-line treatment for advanced ovarian cancer patients. However, chemoresistance is a major obstacle in treating ovarian cancer.

Serous adenocarcinoma (SAC), the most common type of ovarian cancer, usually responds well to initial platinum-based chemotherapy, although it will recur and ultimately develop drug resistance. Clear cell carcinoma (CCC), the second most common type in Japan, is often resistant to initial platinum-based chemotherapy [1]. Regardless of whether the resistance is acquired or primary, more promising therapeutic strategies are necessary to overcome chemoresistance and improve the prognosis of ovarian cancer patients.

Recent studies have suggested that cancer stem cells (CSCs) are, at least in part, responsible for chemoresistance in many types of cancers including ovarian cancer [reviewed in [2]]. CSCs are a subpopulation of tumor cells, which are characterized by a self-renewal capacity and ability to differentiate into distinct cell types. The emergence of CSCs occurs at least partly as a result of epithelial-mesenchymal transition (EMT), a process essential for embryonic development, which is induced during cancer progression and crucial for cancer metastasis. CSCs possess the self-renewal feature of normal stem cells, and similar signaling pathways regulate self-renewal of CSCs and normal stem cells [3]. One such pathway involves telomerase reverse transcriptase (TERT), the rate-limiting catalytic subunit of telomerase, which is expressed in the majority of cancers. Recent evidence indicates that TERT regulates stem cell traits in a telomere length-independent manner. For example, TERT activates quiescent epidermal stem cells *in vivo* in a manner independent of the intrinsic RNA component of the telomerase enzyme TERC [4]. In addition, together with the SWItch-Sucrose NonFermentable (SWI-SNF) complex protein brahma-related gene 1 (BRG1), TERT acts as a transcriptional modulator of the Wnt/β-catenin signaling pathway, contributing to self-renewal and proliferation during development [5]. More recently, accumulating evidence indicates that TERT also operates in CSCs and promotes EMT and CSC-like traits. Specifically, overexpression of human TERT (hTERT) results in an enhanced sphere-forming capacity, increased expression of EMT/CSC markers, and increased *in vivo* tumorigenesis caused by hTERT interacting with β-catenin and enhancing its transcriptional activity [6]. Conversely, suppression of hTERT expression results in a decreased sphere-forming capacity and decreased expression of the CSC marker

CD44 [7]. This function of hTERT in promotion of EMT and CSC-like traits appears to be independent of its telomerase activity [6]. Indeed, we have reported that hTERT in a complex with BRG1 and the nucleolar GTP-binding protein nucleostemin (NS) (TBN complex) participates in maintenance of CSCs. Moreover, we found that overexpression of the TBN complex enhances tumorigenicity and expression of EMT/CSC markers in an hTERT-dependent manner but in a telomere length-independent manner [8]. The exact telomerase-independent mechanisms by which the TBN complex regulates CSCs remain elusive. One possible mechanism is via the RNA-dependent RNA polymerase (RdRP) activity of hTERT [9]. RdRP induces RNA interference through production of double-stranded RNAs from single-stranded template RNAs and regulates the assembly of heterochromatin and mitotic progression [10]. Similar to RdRPs in model organisms, we found that the RdRP activities of the TBN complex are high in mitotic cells, and suppression of the TBN complex results in mitotic arrest [11].

To address chemoresistance, therapeutic strategies targeting EMT and CSCs are increasingly attracting attention. Recently, because eribulin mesylate (eribulin) was reported to inhibit metastasis by reversing EMT [12], we speculated that eribulin might target CSCs. Eribulin is a non-taxane inhibitor of microtubule dynamics [13], which induces irreversible mitotic blockade, leading to persistent inactivation of Bcl-2 and subsequent apoptosis [14]. In the United States, eribulin has been approved for treatment of metastatic breast cancer after at least two treatment regimens including an anthracycline and a taxane. Furthermore, eribulin is approved for treatment of inoperable or recurrent breast cancer in Japan.

In this study, we found that eribulin effectively inhibited growth of platinum-resistant ovarian cancer cells. Eribulin-sensitive cells showed enhanced CSC-like characteristics and high hTERT expression. Suppression of hTERT expression resulted in decreased sensitivity to eribulin. Moreover, eribulin inhibited the RdRP activity of hTERT *in vitro*, demonstrating that hTERT is a direct target of eribulin.

Results

Eribulin inhibits growth of cisplatin-resistant ovarian adenocarcinoma cell lines

Fourteen ovarian adenocarcinoma cell lines were investigated for sensitivity to cisplatin [cis-diamminedichloroplatinum(II)], including six SAC cell lines (PEO1, PEO4, PEO14, PEO23, OVKATE, and OVSAHO), six CCC cell lines (RMG-I, ES-2, OVISE, OVMANA, OVTOKO, and TOV21G), and two undifferentiated/unclassified adenocarcinoma cell lines (OV-CAR-3 and A2780) (Table S1). As shown in Figure 1A, OVKATE, RMG-I, PEO4, and PEO23 cells were particularly resistant to cisplatin, presumably via different mechanisms. OVKATE cells have been previously reported as resistant to platinum agents with elevated expression of glutathione-S-transferase, a drug-resistance marker [15]. RMG-I cells are also resistant to cisplatin, which involves the extracellular signal-regulated kinase (ERK) pathway [16]. PEO4 and PEO23 cells were derived from the same patients as PEO1 and PEO14 cells, respectively, after development of clinical chemoresistance, and are therefore platinum resistant [17]. BRCA2 mutation has been found to contribute to platinum resistance in PEO4 cells [18].

We screened a series of known anti-cancer compounds for growth inhibition of platinum-resistant ovarian cancer cell lines. We found that eribulin, a mitotic inhibitor that suppresses microtubule dynamics [13], inhibited growth of RMG-I, PEO23, and PEO4 cells (Figure 1B). Strikingly, eribulin was not as effective in some of the cisplatin-sensitive cell lines such as OVTOKO, PEO14, and TOV21G (Figure 1A and 1B). For further characterization, we defined eight cell lines with an IC_{50} of <100 nM for eribulin as "eribulin-sensitive" (Eribulin S) and six cell lines with an IC_{50} of >100 nM for eribulin as "eribulin-resistant" (Eribulin R).

Eribulin-sensitive cell lines show a higher sphere-forming capacity

CSCs are thought to be responsible for chemoresistance, and CSCs have been reported to contribute to cisplatin resistance in several types of cancer [19]. Moreover, it was recently reported that eribulin reverses EMT [12], a phenotype that is highly related to CSCs. Therefore, we investigated whether eribulin-sensitive cells possess an enhanced CSC-like phenotype. Because a sphere-forming capacity is a CSC-like characteristic, we performed sphere formation assays under serum-free conditions, and found that eribulin-sensitive cell lines showed high sphere formation efficiency (Figure 2A and 2B). The sphere formation efficiency of Eribulin S cell lines was significantly higher than that of Eribulin R cell lines (Figure 2C, $p = 0.0013$), suggesting that eribulin-sensitive cell lines possess enhanced CSC-like characteristics.

Since we have recently demonstrated that NS together with hTERT and BRG1 maintains CSCs [8] and we and others have also demonstrated that NS is a useful CSC marker [20–22], we investigated the expression of BRG1 and NS in Eribulin S and Eribulin R cell lines. The protein expression level of BRG1 was significantly higher in Eribulin S cell lines (Figure 2D and 2E, $p = 0.0189$), while only a modest tendency of higher level of NS in Eribulin S cell lines was observed (Figure 2D and 2E, $p = 0.1216$). We did not detect a difference in the expression level of CD133 or CD44 (Figure S1), the cell surface markers implied in some CSCs [23].

Eribulin S cells express higher levels of hTERT protein

Overexpression of hTERT results in an enhanced sphere-forming capacity in gastric cancer cells [6]. Conversely, suppression of hTERT expression results in a decreased sphere-forming capacity in breast cancer cells [7]. Therefore, we determined whether the ovarian cancer cells with a higher sphere-forming capacity express a higher level of hTERT. We observed a tendency in cell lines with high sphere-forming efficiency, such as RMG-I, PEO23, and A2780, to express relatively high levels of hTERT protein, while cell lines with low sphere-forming efficiency, such as TOV21G, OVTOKO, and OVMANA, expressed low levels of hTERT protein, as demonstrated by enzyme-linked immunosorbent assay (ELISA) (Figure 3A). The high level of hTERT expression in RMG-I cells can be accounted for by a gain-of-function mutation (-124 G>A) in the hTERT promoter region (Table S1 and Figure S2). This cancer-specific mutation was recently reported in melanoma and several other types of cancer [24–27], which creates new binding motifs for E-twenty six/ternary complex factors (ETS/TCF) and thus contributes to upregulated hTERT transcription [24,25].

We found that Eribulin S cell lines expressed higher levels of hTERT protein than those in Eribulin R cell lines (Figure 3B, $p = 0.008$).

Suppression of hTERT expression results in decreased sensitivity to eribulin

The correlation between hTERT expression and eribulin sensitivity led us to postulate that eribulin inhibits growth of

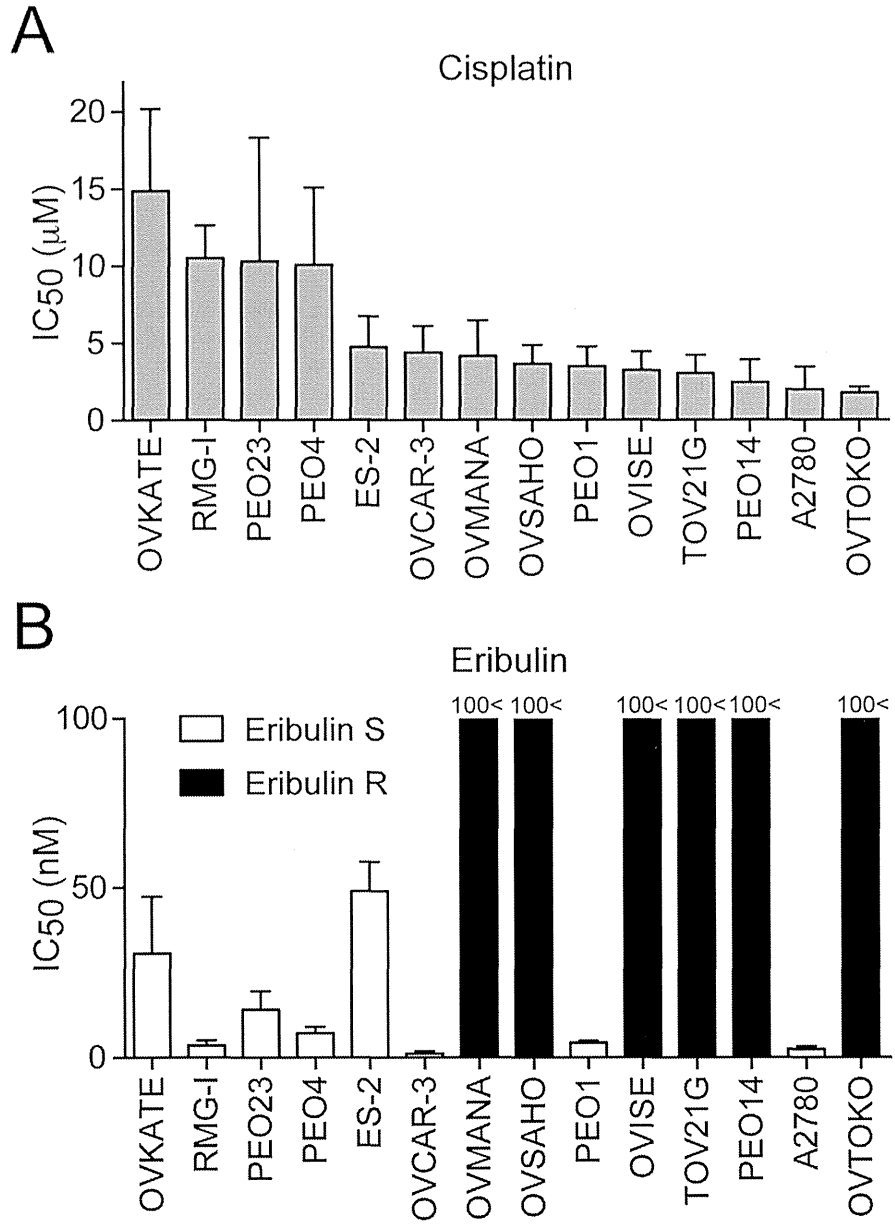

Figure 1. Eribulin inhibits growth of cisplatin-resistant ovarian cancer cells. Cells were treated with cisplatin or eribulin for 72 h, and then cell viability was determined by MTT assays. (A) Mean IC_{50} values for cisplatin (μM). (B) Mean IC_{50} values for eribulin (nM). Eribulin-sensitive (Eribulin S) cell lines are shown as open bars, and eribulin-resistant (Eribulin R) cell lines are shown as closed bars. Error bars represent the SD of at least three independent experiments.
doi:10.1371/journal.pone.0112438.g001

ovarian cancer cells via inhibition of hTERT. To test this hypothesis, we examined whether suppression of hTERT expression in ovarian cancer cells leads to decreased sensitivity to eribulin. Two independent hTERT-specific siRNAs were introduced into A2780 cells, and sensitivity to eribulin was compared with cells expressing control siRNA. As expected, cells expressing hTERT siRNAs showed decreased sensitivity to eribulin (Figure 4A). TERT siRNA1 showed a tendency of stronger suppression of hTERT expression than TERT siRNA2 as demonstrated by ELISA (Figure 4B). This finding may explain why cells expressing TERT siRNA1 tended to be less sensitive to eribulin than those expressing TERT siRNA2 (Figure 4A). Similar results were obtained in ES-2 cells (Figure 4C and 4D). These results suggest that hTERT might be a direct target for eribulin.

Eribulin inhibits RdRP activity of hTERT *in vitro*

It is widely believed that any effect of hTERT suppression is mediated by telomere shortening. However, because we observed decreased sensitivity to eribulin in a relatively short period (Figure 4, 96 h after transfection of siRNA against hTERT), we speculated that this effect is independent of the telomere maintenance function of hTERT. Moreover, the function of hTERT in promotion of EMT and CSC-like traits is independent of its telomerase activity [6]. Together with our recent report showing that hTERT has an RdRP activity independent of telomere maintenance [9], we investigated whether eribulin directly targets hTERT-RdRP activity. We monitored the inhibitory effect of eribulin on hTERT-RdRP activity using an

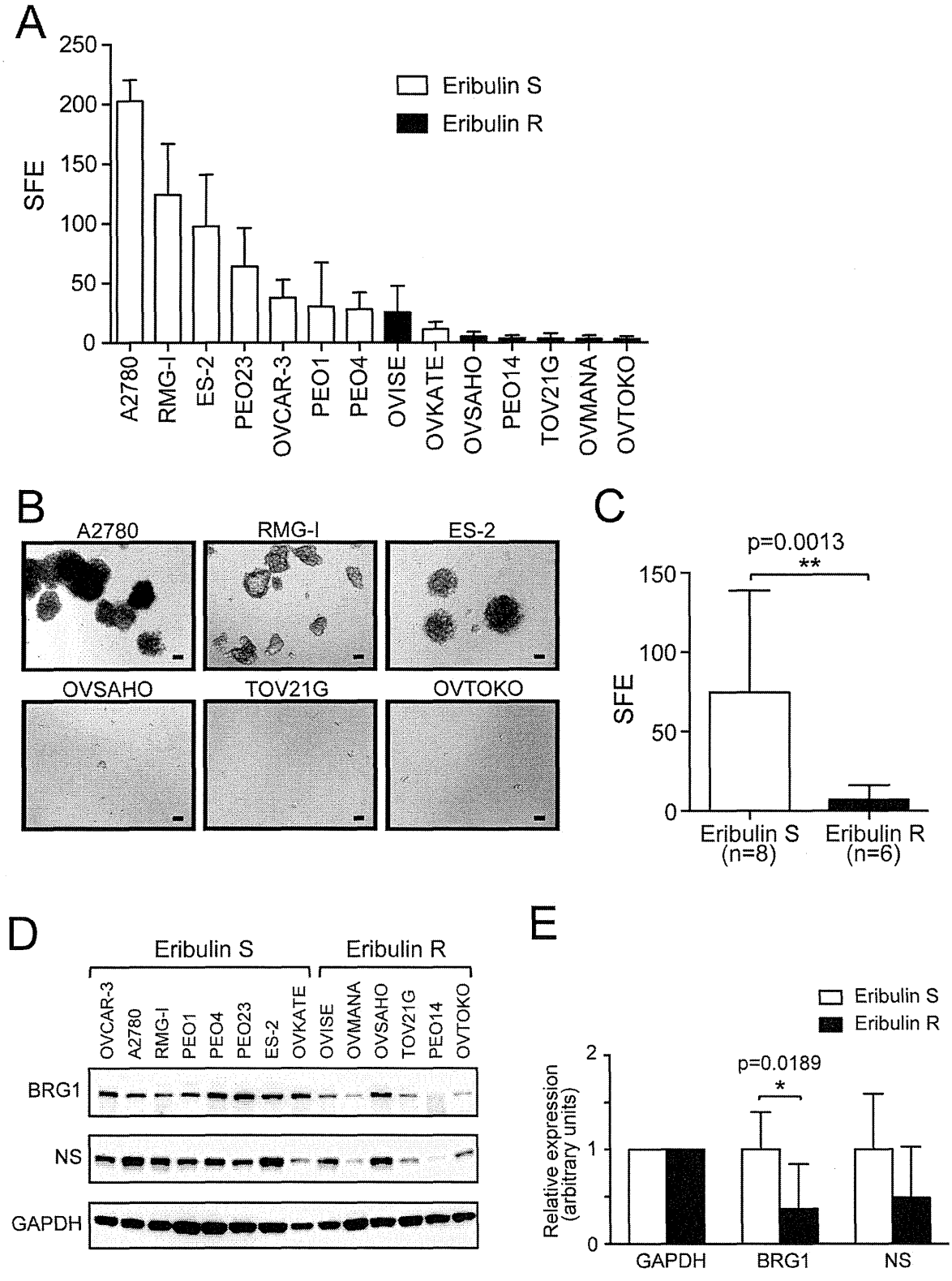

Figure 2. Eribulin-sensitive ovarian cancer cells show high sphere formation efficiency and higher BRG1 expression. (A) Sphere formation efficiency (SFE) of each cell line was indicated per 1,000 cells. Eribulin S cell lines are shown as open bars, and Eribulin R cells are shown as closed bars. Each experiment was performed at least three times, and mean values ± SD are indicated. (B) Morphology of tumorspheres under serum-free conditions. Representative images of spheres formed by A2780, RMG-I, ES-2, OVSAHO, TOV21G, and OVTOKO cells are shown. Scale bar = 50 μm. (C) The mean SFE of Eribulin S cell lines (n = 8) and Eribulin R cell lines (n = 6) shown in (A). Error bars indicate SD. (D) The level of BRG1 and NS protein expression was detected by immunoblotting. GAPDH expression was shown as loading control. (E) Signals in (D) were quantified with ImageJ software and normalized to GAPDH signal. The mean values of relative expression level ± SD are indicated.
doi:10.1371/journal.pone.0112438.g002

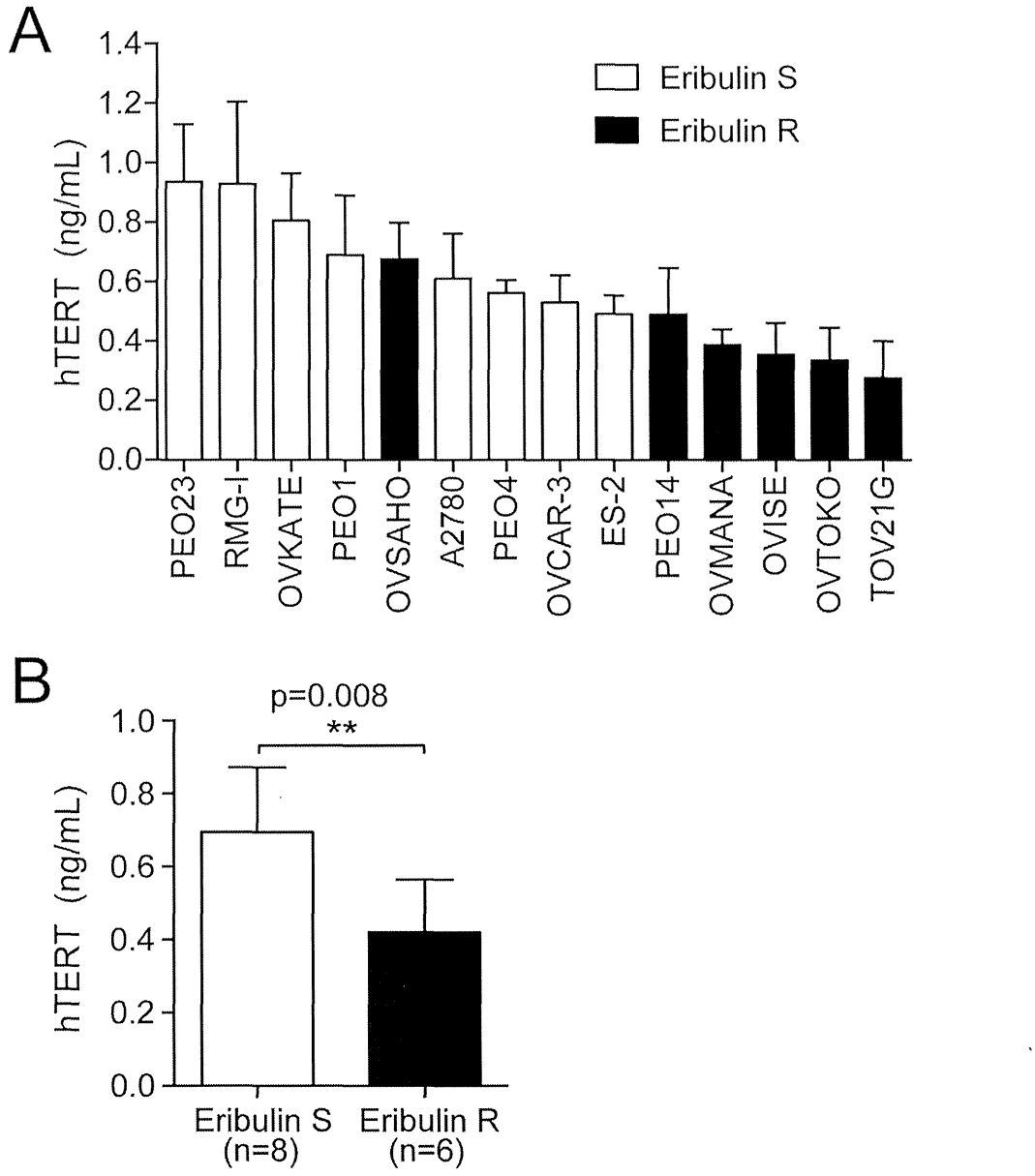

Figure 3. Eribulin-sensitive ovarian cancer cells express higher levels of hTERT protein. (A) The level of hTERT protein expression was determined by ELISA (indicated as ng/ml). Eribulin S cell lines are shown as open bars, and Eribulin R cells are shown as closed bars. Each experiment was performed at least three times, and mean values ± SD are indicated. (B) The mean hTERT level of Eribulin S cell lines (n = 8) and Eribulin R cell lines (n = 6) shown in (A). Error bars indicate SD.
doi:10.1371/journal.pone.0112438.g003

in vitro RdRP assay [11], and found that eribulin inhibited hTERT-RdRP activity *in vitro* at a concentration of 50 μM (Figure 5A). The same concentration of eribulin did not inhibit the telomerase activity of hTERT as shown by telomeric repeat amplification protocol (TRAP) assay (Figure 5B). These results suggest that the effects of eribulin on hTERT are not mediated via telomerase activity, but via RdRP activity. Interestingly, another mitotic inhibitor, paclitaxel, a representative taxane, did not inhibit RdRP activity (Figure 5C), suggesting that eribulin has a specific inhibitory effect on hTERT-RdRP activity.

Discussion

Among gynecological cancers, ovarian cancer is the leading cause of death. In particular, resistance to conventional platinum-based chemotherapy has been a barrier in the improvement of prognoses for ovarian cancer patients, and new therapeutic strategies are urgently required. Here, we found that eribulin was effective to inhibit growth of platinum-resistant ovarian cancer cells. Effects of eribulin were correlated with hTERT expression levels (Figure 3), and suppression of hTERT expression resulted in decreased sensitivity to eribulin (Figure 4), suggesting that hTERT could be a target of eribulin in these cells. Indeed, eribulin inhibited the RdRP activity but not the reverse transcriptase activity of hTERT *in vitro* (Figure 5).

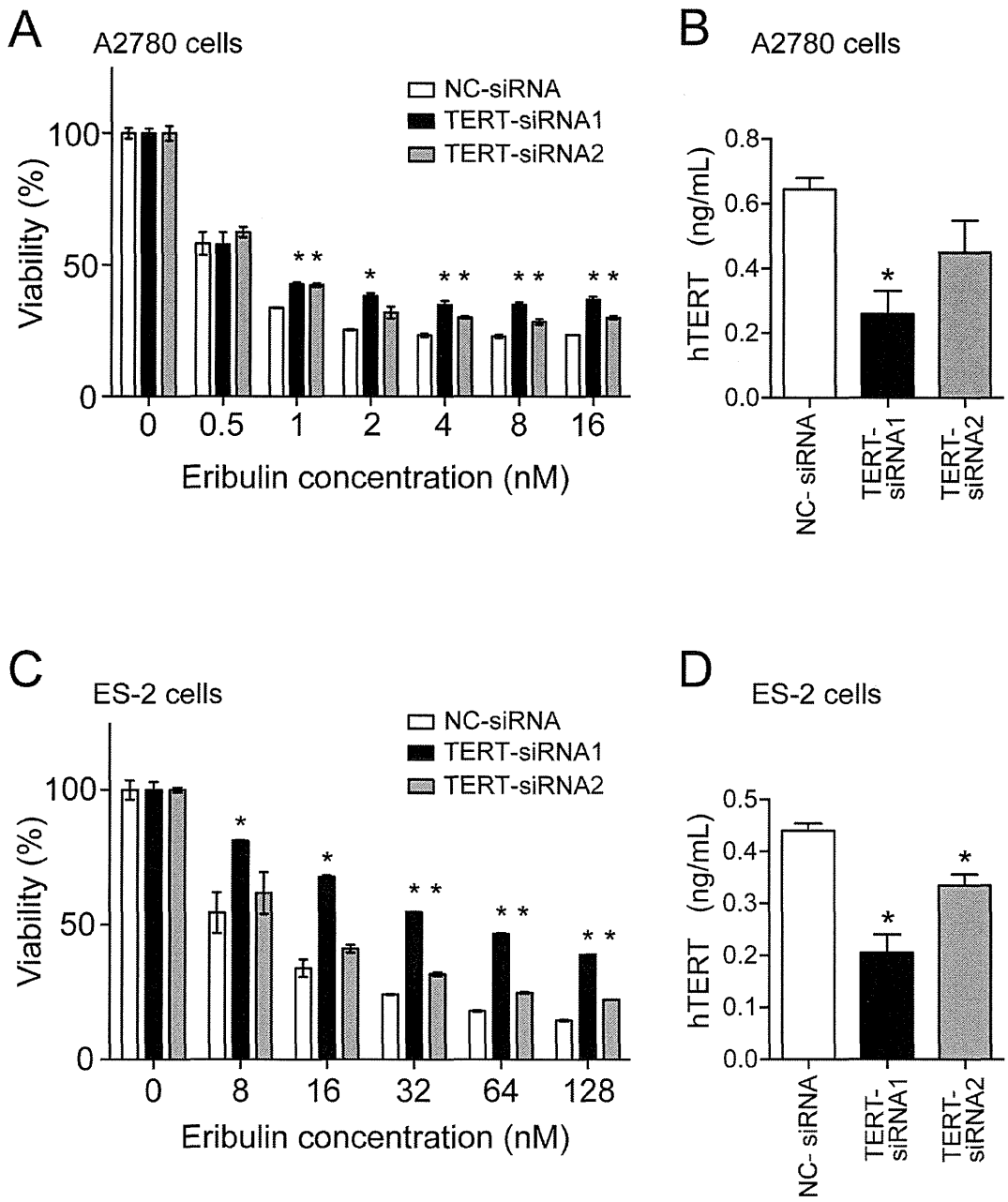

Figure 4. Suppression of hTERT expression by siRNA results in decreased sensitivity to eribulin. (A) A2780 cells expressing control siRNA (open bars), TERT siRNA1 (closed bars), or TERT siRNA2 (shaded bars) were treated with eribulin for 72 h, and then cell viability was determined by MTT assays. *$p<0.05$ vs. cells expressing control siRNA. (B) The level of hTERT protein expression in A2780 cells expressing control siRNA (open bars), TERT siRNA1 (closed bars), or TERT siRNA2 (shaded bars) was determined by ELISA (indicated as ng/ml). (C and D) The experiments described in (A and B) were performed in the same manner using ES-2 cells expressing control siRNA (open bars), TERT siRNA1 (closed bars), or TERT siRNA2 (shaded bars). *$p<0.05$ vs. cells expressing control siRNA.
doi:10.1371/journal.pone.0112438.g004

CSCs and hTERT

CSCs are thought to be involved in chemoresistance, and several pathways have been found to contribute to the promotion or maintenance of CSCs. We and others have shown that hTERT plays an important role in promotion and maintenance of CSCs in telomere maintenance-independent manners [6–8]. Eribulin effectively inhibited growth of platinum-resistant cells (Figure 1). Eribulin-sensitive cells exhibited higher hTERT expression (Figure 3) and a higher sphere-forming capacity (Figure 2), suggesting that these cells have enhanced CSC-like characteristics, possibly due to the high levels of hTERT protein. Consistently, eribulin-sensitive cells exhibited higher BRG1 expression (Figure 2), another component of the TBN complex that maintains CSCs. We did not detect a significant difference in the expression of CD133 or CD44 (Figure S1). Although CD133 and CD44 are thought to be indicative of CSCs in some types of cancer, it remains to be elucidated what markers are appropriate for CSCs in ovarian cancers [23].

Because telomere maintenance by telomerase is indispensable for infinite proliferation of malignant cells, efforts have been made

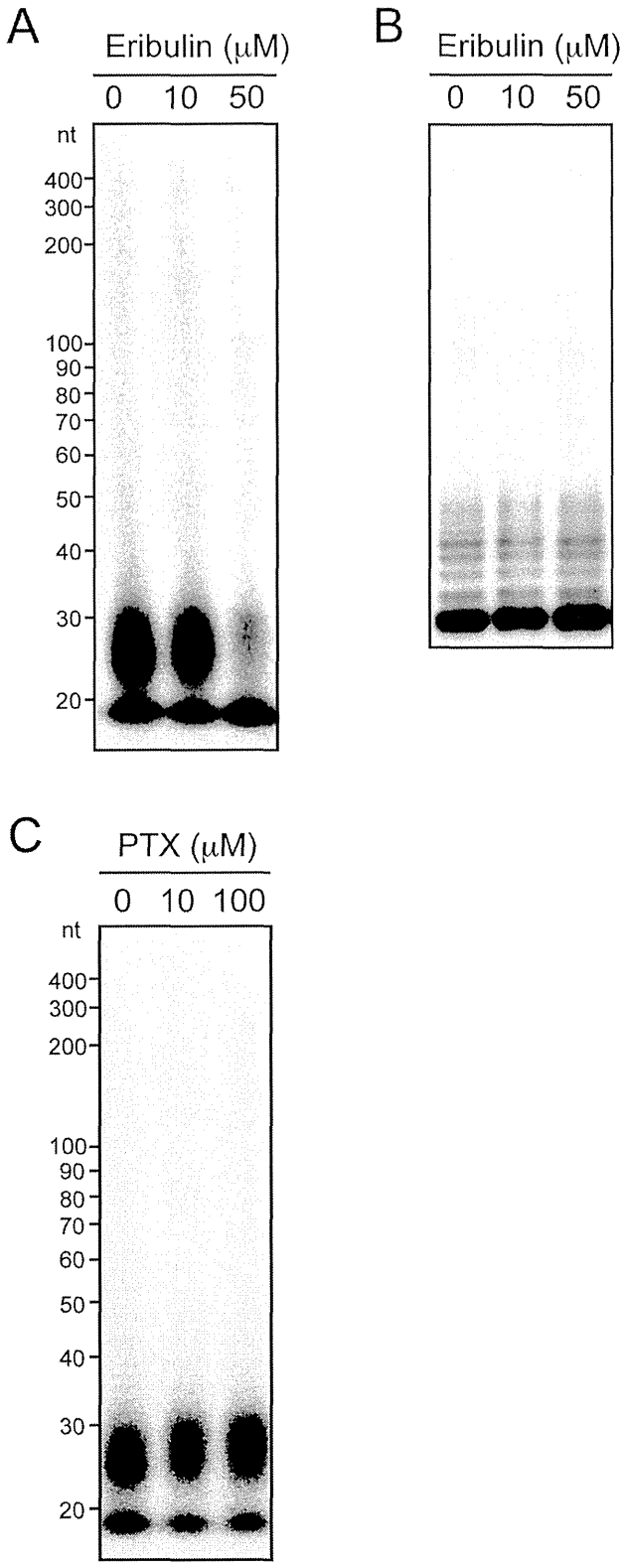

Figure 5. Eribulin inhibits RdRP activity but not telomerase activity of hTERT. (A) RdRP activity of hTERT immune complexes prepared from HeLa cells arrested in the mitotic phase was assayed without or with 10 and 50 μM eribulin. (B) Telomerase activity in HeLa cell extracts was assayed without or with 10 and 50 μM eribulin. (C) RdRP activity of hTERT immune complexes was assayed without or with 10 and 100 μM paclitaxel (PTX).
doi:10.1371/journal.pone.0112438.g005

to develop anticancer therapeutics targeting telomerase. Recent studies indicate that TERT plays functional roles beyond telomere maintenance. Indeed, the function of TERT to activate normal quiescent stem cells or CSC-like traits has been shown to be independent of its telomerase activity [4,6,28]. We have also found that the TBN complex maintains CSCs in a telomere length-independent manner [8]. It is possible that this telomerase-independent mechanism is mediated by the RdRP activity of TERT, because the TBN complex itself is responsible for the RdRP activity and is involved in heterochromatin regulation and mitotic progression [11]. We speculate that the RdRP activity of hTERT is involved in gene expression through heterochromatin regulation in cancer cells, and it could be a novel anticancer therapeutic target. Whether RdRP activity is prerequisite for hTERT function in the promotion of CSCs remains to be determined.

Eribulin and hTERT

Eribulin binds to microtubule plus ends and inhibits the growth phase of microtubule dynamics [29]. Recently, eribulin was shown to reverse EMT by downregulating transforming growth factor-β (TGF-β)-induced Smad phosphorylation [12]. Smad proteins bind to microtubules in the absence of TGF-β and TGF-β triggers dissociation from microtubules and phosphorylation of Smad proteins [30]. Yoshida *et al.* speculated that eribulin inhibits Smad phosphorylation possibly by suppressing Smad dissociation from microtubules [12]. Because we have recently demonstrated that hTERT localizes to mitotic spindles and centromeres during mitosis [11], it is also possible that eribulin inhibits hTERT functions by interfering with the interaction between hTERT and microtubules. Eribulin improves overall survival of patients with metastatic breast cancer, who had prior anthracycline- and taxane-based chemotherapy [31]. A taxane drug, paclitaxel, did not inhibit the RdRP activity of hTERT (Figure 5C), providing one of the potential molecular bases for the different clinical outcomes of taxanes and eribulin. The exact mechanism by which eribulin inhibits hTERT function is yet to be understood.

hTERT as a biomarker

It is important to identify biomarkers to predict responses to anticancer therapies. By determination of hTERT levels in clinical specimens, patients who are likely to respond well to eribulin may be identified before they receive chemotherapy. In particular, an ELISA would be able to measure hTERT levels in clinical practice.

In summary, we found that eribulin inhibits RdRP activity of hTERT, which may contribute to chemoresistance in ovarian cancer by maintaining CSCs. Eribulin inhibited the growth of ovarian cancer cells with high hTERT expression and strong platinum resistance, suggesting it may be a promising therapeutic agent for chemoresistant ovarian cancer. Moreover, hTERT may be a useful biomarker to predict clinical responses to eribulin.

Materials and Methods

Cell lines

RMG-I [32], OVMANA [33], OVTOKO [34], OVISE [34], OVSAHO [33], and OVKATE [33] cells were obtained from the Japanese Collection of Research Bioresources Cell Bank. OV-CAR-3 cells [35] were obtained from the RIKEN BioResource Center. PEO1, PEO4, PEO14, PEO23 [17], and A2780 [36] cells were purchased from the European Collection of Cell Cultures, and TOV21G [37] and ES-2 [38] cells were purchased from the American Type Culture Collection. RMG-I cells were cultured in

Ham's F12 medium supplemented with 10% fetal bovine serum, ES-2 cells in McCoy's 5a medium supplemented with 10% fetal bovine serum, TOV21G cells in MCDB105/Medium 199 (1:1) supplemented with 10% fetal bovine serum, and HeLa cells in Dulbecco's modified Eagle's medium (DMEM) supplemented with 10% fetal bovine serum. All other cell lines (A2780, OVCAR-3, OVMANA, OVTOKO, OVISE, OVSAHO, OVKATE, PEO1, PEO4, PEO14, and PEO23) were cultured in RPMI-1640 medium supplemented with 10% fetal bovine serum and 1 mM sodium pyruvate (Gibco, Grand Island, NY, USA).

Compounds

Cisplatin was purchased from Sigma-Aldrich (St Louis, MO, USA), paclitaxel was purchased from Wako (Osaka, Japan), and eribulin (Halaven) was purchased from Eisai Co., Ltd (Tsukuba, Japan).

MTT assay

Cells (5,000–10,000 per well) were seeded in 96-well plates and then treated with cisplatin or eribulin after 24 h. At 72 h of treatment, an MTT proliferation assay (Cell Proliferation Kit I MTT, Roche Diagnostics, Mannheim, Germany) was performed according to the manufacturer's protocol. Briefly, 10 μl MTT labeling reagent was added to each well, followed by 4 h of incubation. Then, 100 μl solubilization solution was added to each well, followed by overnight incubation. The reaction product was quantified by measuring the absorbance at 570 and 690 nm using a microplate reader (Viento 808, BioTek, Winooski, VT, USA). Cell viability was determined by comparisons to untreated cells.

Sphere formation assay

Single cells were seeded in 96-well ultra low attachment plates (Corning Inc, Corning, NY, USA) at 100–1,000 cells/100 μl medium in each well. Cells were grown in serum-free DMEM/F12 medium (Gibco) supplemented with 20 ng/ml basic fibroblast growth factor (Wako), 20 ng/ml epidermal growth factor (Wako), and B27 supplement (Gibco). Cultures were supplemented with 25 μl of fresh medium every 3–4 days, and the number of spheres was counted on days 7 and 14. Microscopic images were obtained with a CKX41 inverted microscope and DP21 digital camera (Olympus, Tokyo, Japan).

Immunoblotting

Cells were lysed in radioimmunoprecipitation assay (RIPA) buffer containing 1% NP-40, 1 mM EDTA, 50 mM Tris-HCl (pH 7.4) and 150 mM NaCl. After sonication and centrifugation of the lysates, proteins (20 μg) were subjected to SDS-PAGE in 7.5% poly-acrylamide gels, followed by immunoblot analysis. The following antibodies were used: anti-BRG1 (a gift from Dr. Tsutomu Ohta, National Cancer Center, Japan), anti-NS (A300–600A; Bethyl Laboratories, Montgomery, TX, USA), anti-GAPDH (3H12; Medical & Biological Laboratories (MBL), Nagoya, Japan), anti-CD133 (W6B3C1; Miltenyi Biotec, Bergisch Gladbach, Germany) and anti-CD44 (2C5; R&D Systems, Minneapolis, MN, USA). Signals were detected by LAS-3000 (Fujifilm, Tokyo, Japan), quantified with ImageJ software (National Institutes of Health, USA) and normalized using GAPDH loading control.

hTERT ELISA

The hTERT ELISA employed a rabbit anti-hTERT polyclonal antibody as the capture antibody (MBL), and a mouse anti-hTERT monoclonal antibody (mAb) (clone 2E4-5) as the detection antibody (MBL code no. 5340, Ab-Match Assembly Human TERT Kit). The 2E4-5 antibody was generated against recombinant hTERT as an immunogen as described previously [11]. Cells were lysed in RIPA buffer. After sonication and centrifugation of the lysates, 100 μg total protein (100 μl in volume) was added to each well of a 96-well plate (MBL code no. 5310, Ab-Match Universal Kit). The ELISA was performed according to the manufacturer's instructions. Absorbances at 450 and 630 nm were measured by a microplate reader. Each experiment was performed at least three times, and mean values were calculated.

TERT promoter mutation analysis

Genomic DNA was extracted from ovarian cancer cell lines using a Blood and Cell Culture DNA Kit (Qiagen, Hilden, Germany) according to the manufacturer's protocol. The *TERT* promoter region (−146 to −124-bp upstream from the start codon) was amplified by PCR using KOD FX (Toyobo, Osaka, Japan) and the following primers: 5′-GTCCTGCCCCTTCACCTT-3′ and 5′-CAGCGCTGCCT-GAAACTC-3′ [25]. PCR was performed under the following conditions: 40 cycles of 98°C for 10 s, 55°C for 30 s, and 68°C for 60 s. Purified PCR products were sequenced by Sanger sequencing.

Transfection of siRNA

Cells were transfected with siRNA by Lipofectamine RNAiMAX (Invitrogen) and then seeded at 5,000–10,000 cells per well in 96-well plates. At 24 h after transfection, the cells were treated with eribulin, and an MTT assay was performed after 72 h of treatment. For the ELISA, $2–5.0\times10^6$ cells transfected with siRNA were plated in a 10-cm petri dish, and then collected after 48 h of incubation. hTERT siRNA1 and hTERT siRNA2 have been described previously [8]. The negative control siRNA (MISSION siRNA Universal Negative Control; Sigma-Aldrich) was also used.

IP-RdRP assay

In order to detect RdRP activity *in vitro*, the hTERT immune complex was isolated by mAb against hTERT. An IP-RdRP assay has been established in mitotically arrested HeLa cells [11]. Therefore, HeLa cells were used for this assay. To synchronize HeLa cells undergoing mitosis, the cells were cultured in medium containing 2.5 mM thymidine (Nacalai Tesque, Kyoto, Japan) for 24 h. At 6 h after release, the cells were incubated in medium containing 0.1 μg/ml nocodazole (Sigma-Aldrich) for 14 h. After shaking gently, mitotic cells were retrieved. The IP-RdRP assay was performed as described previously [11].

TRAP assay

A TRAP assay was used to detect telomere specific reverse transcriptase activity as described previously [39].

Statistical analysis

Statistical analyses were performed with GraphPad Prism 6 (GraphPad Software, La Jolla, CA, USA). The Student's t-test or Mann Whitney test was used. Two-sided p-values of <0.05 were considered statistically significant.

Supporting Information

Figure S1 CD133 and CD44 expression in Eribulin S and Eribulin R ovarian cancer cells. (A) The level of CD133 and CD44 protein expression was detected by immunoblotting.

Since the data was obtained in the same experiment as Figure 2 panel D, GAPDH gel was identical with Figure 2 panel D. (B) Signals in (A) were quantified with ImageJ software and normalized to GAPDH signal. The mean values of relative expression level ± SD are indicated.
(TIF)

Figure S2 ES-2 and RMG-I cells possess hTERT promoter mutations. The hTERT promoter was sequenced in each cell line. ES-2 cells harbor a -138/-139 GG>AA mutation as described previously [27], and RMG-I cells harbor a -124 G>A mutation. The wild-type sequences of the corresponding regions from OVKATE and OVSAHO cells are shown as controls.
(TIF)

Table S1 Ovarian cancer cell lines used in this study.
(DOCX)

Acknowledgments

We thank Dr. Tsutomu Ohta for the gift of anti-BRG1 antibody, Dr. Koichi Ichimura for technical assistance with promoter mutation analysis, and MBL for their assistance in establishing the ELISA kit for hTERT detection.

Author Contributions

Conceived and designed the experiments: SY KM. Performed the experiments: SY YM M. Yasukawa. Analyzed the data: SY YM. Contributed reagents/materials/analysis tools: TK M. Yoshida. Contributed to the writing of the manuscript: SY YM KM.

References

1. Takano M, Tsuda H, Sugiyama T (2012) Clear cell carcinoma of the ovary: is there a role of histology-specific treatment? J Exp Clin Cancer Res 31: 53.
2. Singh A, Settleman J (2010) EMT, cancer stem cells and drug resistance: an emerging axis of evil in the war on cancer. Oncogene 29: 4741–4751.
3. Pardal R, Clarke MF, Morrison SJ (2003) Applying the principles of stem-cell biology to cancer. Nat Rev Cancer 3: 895–902.
4. Sarin KY, Cheung P, Gilison D, Lee E, Tennen RI, et al. (2005) Conditional telomerase induction causes proliferation of hair follicle stem cells. Nature 436: 1048–1052.
5. Park JI, Venteicher AS, Hong JY, Choi J, Jun S, et al. (2009) Telomerase modulates Wnt signalling by association with target gene chromatin. Nature 460: 66–72.
6. Liu Z, Li Q, Li K, Chen L, Li W, et al. (2013) Telomerase reverse transcriptase promotes epithelial-mesenchymal transition and stem cell-like traits in cancer cells. Oncogene 32: 4203–4213.
7. Chung SS, Aroh C, Vadgama JV (2013) Constitutive Activation of STAT3 Signaling Regulates hTERT and Promotes Stem Cell-Like Traits in Human Breast Cancer Cells. PLoS One 8: e83971.
8. Okamoto N, Yasukawa M, Nguyen C, Kasim V, Maida Y, et al. (2011) Maintenance of tumor initiating cells of defined genetic composition by nucleostemin. Proc Natl Acad Sci U S A 108: 20388–20393.
9. Maida Y, Yasukawa M, Furuuchi M, Lassmann T, Possemato R, et al. (2009) An RNA-dependent RNA polymerase formed by TERT and the RMRP RNA. Nature 461: 230–235.
10. Martienssen RA, Zaratiegui M, Goto DB (2005) RNA interference and heterochromatin in the fission yeast Schizosaccharomyces pombe. Trends Genet 21: 450–456.
11. Maida Y, Yasukawa M, Okamoto N, Ohka S, Kinoshita K, et al. (2014) Involvement of telomerase reverse transcriptase in heterochromatin maintenance. Mol Cell Biol 34: 1576–1593.
12. Yoshida T, Ozawa Y, Kimura T, Sato Y, Kuznetsov G, et al. (2014) Eribulin mesilate suppresses experimental metastasis of breast cancer cells by reversing phenotype from epithelial-mesenchymal transition (EMT) to mesenchymal-epithelial transition (MET) states. Br J Cancer 110: 1497–1505.
13. Towle MJ, Salvato KA, Budrow J, Wels BF, Kuznetsov G, et al. (2001) In vitro and in vivo anticancer activities of synthetic macrocyclic ketone analogues of halichondrin B. Cancer Res 61: 1013–1021.
14. Towle MJ, Salvato KA, Wels BF, Aalfs KK, Zheng W, et al. (2011) Eribulin induces irreversible mitotic blockade: implications of cell-based pharmacodynamics for in vivo efficacy under intermittent dosing conditions. Cancer Res 71: 496–505.
15. Ohta I, Gorai I, Miyamoto Y, Yang J, Zheng JH, et al. (2001) Cyclophosphamide and 5-fluorouracil act synergistically in ovarian clear cell adenocarcinoma cells. Cancer Lett 162: 39–48.
16. Wang J, Zhou JY, Wu GS (2011) Bim protein degradation contributes to cisplatin resistance. J Biol Chem 286: 22384–22392.
17. Langdon SP, Lawrie SS, Hay FG, Hawkes MM, McDonald A, et al. (1988) Characterization and properties of nine human ovarian adenocarcinoma cell lines. Cancer Res 48: 6166–6172.
18. Sakai W, Swisher EM, Jacquemont C, Chandramohan KV, Couch FJ, et al. (2009) Functional restoration of BRCA2 protein by secondary BRCA2 mutations in BRCA2-mutated ovarian carcinoma. Cancer Res 69: 6381–6386.
19. Vidal SJ, Rodriguez-Bravo V, Galsky M, Cordon-Cardo C, Domingo-Domenech J (2014) Targeting cancer stem cells to suppress acquired chemotherapy resistance. Oncogene 33: 4451–4463.
20. Tamase A, Muraguchi T, Naka K, Tanaka S, Kinoshita M, et al. (2009) Identification of tumor-initiating cells in a highly aggressive brain tumor using promoter activity of nucleostemin. Proc Natl Acad Sci U S A 106: 17163–17168.
21. Kobayashi T, Masutomi K, Tamura K, Moriya T, Yamasaki T, et al. (2014) Nucleostemin expression in invasive breast cancer. BMC Cancer 14: 215.
22. Lin T, Meng L, Li Y, Tsai RY (2010) Tumor-initiating function of nucleostemin-enriched mammary tumor cells. Cancer Res 70: 9444–9452.
23. Medema JP (2013) Cancer stem cells: the challenges ahead. Nat Cell Biol 15: 338–344.
24. Huang FW, Hodis E, Xu MJ, Kryukov GV, Chin L, et al. (2013) Highly recurrent TERT promoter mutations in human melanoma. Science 339: 957–959.
25. Horn S, Figl A, Rachakonda PS, Fischer C, Sucker A, et al. (2013) TERT promoter mutations in familial and sporadic melanoma. Science 339: 959–961.
26. Killela PJ, Reitman ZJ, Jiao Y, Bettegowda C, Agrawal N, et al. (2013) TERT promoter mutations occur frequently in gliomas and a subset of tumors derived from cells with low rates of self-renewal. Proc Natl Acad Sci U S A 110: 6021–6026.
27. Wu RC, Ayhan A, Maeda D, Kim KR, Clarke BA, et al. (2013) Frequent somatic mutations of the telomerase reverse transcriptase promoter in ovarian clear cell carcinoma but not in other major types of gynecologic malignancies. J Pathol 232: 473–481.
28. Choi J, Southworth LK, Sarin KY, Venteicher AS, Ma W, et al. (2008) TERT promotes epithelial proliferation through transcriptional control of a Myc- and Wnt-related developmental program. PLoS Genet 4: e10.
29. Smith JA, Wilson L, Azarenko O, Zhu X, Lewis BM, et al. (2010) Eribulin binds at microtubule ends to a single site on tubulin to suppress dynamic instability. Biochemistry 49: 1331–1337.
30. Dong C, Li Z, Alvarez R Jr, Feng XH, Goldschmidt-Clermont PJ (2000) Microtubule binding to Smads may regulate TGF beta activity. Mol Cell 5: 27–34.
31. Cortes J, O'Shaughnessy J, Loesch D, Blum JL, Vahdat LT, et al. (2011) Eribulin monotherapy versus treatment of physician's choice in patients with metastatic breast cancer (EMBRACE): a phase 3 open-label randomised study. Lancet 377: 914–923.
32. Nozawa S, Tsukazaki K, Sakayori M, Jeng CH, Iizuka R (1988) Establishment of a human ovarian clear cell carcinoma cell line (RMG-I) and its single cell cloning–with special reference to the stem cell of the tumor. Hum Cell 1: 426–435.
33. Yanagibashi T, Gorai I, Nakazawa T, Miyagi E, Hirahara F, et al. (1997) Complexity of expression of the intermediate filaments of six new human ovarian carcinoma cell lines: new expression of cytokeratin 20. Br J Cancer 76: 829–835.
34. Gorai I, Nakazawa T, Miyagi E, Hirahara F, Nagashima Y, et al. (1995) Establishment and characterization of two human ovarian clear cell adenocarcinoma lines from metastatic lesions with different properties. Gynecol Oncol 57: 33–46.
35. Hamilton TC, Young RC, McKoy WM, Grotzinger KR, Green JA, et al. (1983) Characterization of a human ovarian carcinoma cell line (NIH:OVCAR-3) with androgen and estrogen receptors. Cancer Res 43: 5379–5389.
36. Hamilton TC, Young RC, Ozols RF (1984) Experimental model systems of ovarian cancer: applications to the design and evaluation of new treatment approaches. Semin Oncol 11: 285–298.
37. Provencher DM, Lounis H, Champoux L, Tetrault M, Manderson EN, et al. (2000) Characterization of four novel epithelial ovarian cancer cell lines. In Vitro Cell Dev Biol Anim 36: 357–361.
38. Lau DH, Lewis AD, Ehsan MN, Sikic BI (1991) Multifactorial mechanisms associated with broad cross-resistance of ovarian carcinoma cells selected by cyanomorpholino doxorubicin. Cancer Res 51: 5181–5187.
39. Kim NW, Piatyszek MA, Prowse KR, Harley CB, West MD, et al. (1994) Specific association of human telomerase activity with immortal cells and cancer. Science 266: 2011–2015.

BMC Cancer

RESEARCH ARTICLE Open Access

Nucleostemin expression in invasive breast cancer

Takayuki Kobayashi[1,2], Kenkichi Masutomi[3], Kenji Tamura[4], Tomoyuki Moriya[5], Tamio Yamasaki[5], Yasuhiro Fujiwara[4], Shunji Takahashi[2], Junji Yamamoto[5] and Hitoshi Tsuda[1,6*]

Abstract

Background: Recently, the cancer stem cell hypothesis has become widely accepted. Cancer stem cells are thought to possess the ability to undergo self-renewal and differentiation, similar to normal stem cells. Nucleostemin (NS), initially cloned from rat neural stem cells, binds to various proteins, including p53, in the nucleus and is thought to be a key molecule for stemness. NS is expressed in various types of cancers; therefore, its role in cancer pathogenesis is thought to be important. This study was conducted to clarify the clinicopathological and prognostic impact of NS in invasive breast cancers.

Method: The correlation between NS immunoreactivity and clinicopathological parameters was examined in 220 consecutive surgically resected invasive breast cancer tissue samples by using tissue microarrays. The presence of nuclear NS and p53 immunoreactivity in 10% or more of cancer cells was considered as a positive result.

Results: Among the 220 patients, 154 were hormone-receptor (HR)-positive, 22 HER2-positive/HR-negative, and 44 HR-negative/HER2-negative. One hundred and forty-two tumors (64.5%) showed NS positivity, and this positivity was significantly correlated with estrogen receptor (ER) ($P = 0.050$), human epidermal growth factor receptor 2 (HER2) ($P = 0.021$), and p53 ($P = 0.031$) positivity. The patients with NS-positive tumors showed significantly shorter disease-free survival than those with NS-negative tumors. Furthermore, the patient group with NS- and p53-positive tumors showed significantly poorer prognosis than other patient groups. Multivariate analysis showed that NS status was an independent prognostic indicator.

Conclusions: NS may play a significant role in the determination of breast cancer progression in association with p53 alterations. The NS status of patients with luminal and HER2 type breast cancers may be a useful prognostic marker.

Background

Breast cancer is one of the most prevalent diseases worldwide. While most patients with early breast cancers are cured with surgically resection followed by appropriate adjuvant drug and radiation therapy, approximately 30% of these patients experience relapse and develop metastatic disease [1]. In this metastatic stage, tumor cells frequently acquire resistance to various drugs during intensive systemic therapies, and eventually their aggressiveness and growth become uncontrollable. Less than 5% of patients with distant metastatic tumors live for 5 years [2]. Therefore, identification of potential targets with the aim of developing interventional drugs is an important area of research.

The hypothesis that various types of cancers, including breast cancer, are generated by a limited number of cancer stem cells has been widely accepted recently [3]. Cancer stem cells, like normal stem cells, are thought to have two important characteristics: the ability to undergo self-renewal and the ability to undergo differentiation into different cell types [4]. Furthermore, these cells are thought to be inherently resistant to various therapeutic drugs, making the eradication of tumors containing cancer stem cells with the use of the current treatment protocols difficult [5]. To overcome these obstacles, the development of new therapeutic strategies to target cancer stem cells is essential for the management of breast cancer.

* Correspondence: htsuda@ndmc.ac.jp
[1]Department of Basic Pathology, National Defense Medical College, 3-2 Namiki, Tokorozawa, Saitama 359-8513, Japan
[6]Department of Pathology and Clinical Laboratories, National Cancer Center Hospital, 5-1-1 Tsukiji, Chuo-ku, Tokyo 104-0045, Japan
Full list of author information is available at the end of the article

Nucleostemin (NS) is thought to be a key molecule for maintaining "stemness" [6]. NS was initially cloned from rat neural stem cells and was found to contain two GTP-binding motifs and an N-terminal basic domain, which is essential for binding to p53 [6]. NS accumulates mainly in the nucleoli and moves to the nucleoplasm after binding with GTP. Interaction of NS with a multitude of proteins in the nucleoplasm, including p53, may play a significant role in self-renewal, cell cycle regulation, apoptosis, and cell proliferation [7].

NS is expressed in central nervous system stem cells, embryonic stem cells, and primitive cells in the bone marrow and testes [6]. Furthermore, various types of cancers, including the following, have been reported to express NS: squamous cell carcinomas of the uterine cervix; head, neck, esophagus, and renal cell carcinomas; and prostate cancer [8-13]. Moreover, recent evidence indicates that NS is involved in maintaining cancer stem cells [14,15]. These findings suggest that NS may also play an important role in cancer pathogenesis as well as in cancer stem cell maintenance. However, no clinical study has investigated the role of NS in breast cancer.

If NS is expressed in breast cancer stem cells and its expression is correlated with disease progression in breast cancer, it may serve as a powerful prognostic marker for clinical use. To test this hypothesis, we investigated the expression of NS in surgically resected invasive breast cancer specimens from 220 patients by using immunohistochemistry. Furthermore, we examined the prognostic implication of the combination status of NS and p53 and the significance of NS expression status among the three biological subtypes of breast tumors: (a) hormone-receptor (HR) positive (luminal type); (b) human epidermal growth factor receptor 2 (HER2) positive (HER2 type); and (c) HR negative and HER2 negative (triple negative).

Methods

Patients and tumor specimens

The patient cohort used in the present study was the same as the cohort reported in our previous study [16]. Briefly, formalin-fixed paraffin-embedded tissue blocks of invasive breast cancer specimens from 220 consecutive patients were used to construct tissue microarrays (TMAs). All patients with unilateral invasive breast carcinoma underwent mastectomy or breast-conserving surgery at the National Defense Medical College (NDMC) Hospital, Tokorozawa, Japan from 1995 through 1999. These patients had a median follow-up of 74 months after surgery (range, 1–151 months), during which 58 patients experienced relapse. Of the 220 patients, 218 were female patients and 2 were male patients; 101 (45.9%) patients had lymph node metastasis and 8 (3.6%) had distant metastasis at the time of breast cancer diagnosis. In most cases, patients with hormone receptor-positive tumors at the time of diagnosis were prescribed adjuvant endocrine therapy (e.g., tamoxifen, toremifene, fadrozole, or LHRH analogues) for two or more years. The patients with a large tumor and/or four or more lymph node metastases received one of the following adjuvant chemotherapy regimens: cyclophosphamide-epirubicin-5-fluorouracil (CEF), cyclophosphamide-adriamycin-5-fluorouracil (CAF), cyclophosphamide-methotrexate-5-fluorouracil (CMF), and oral fluoropyrimidines. Detailed patient and disease characteristics are documented in Table 1. Clinicopathological data were retrospectively obtained from medical records [16].

This study was approved by the Medical Ethical Committee of National Defense Medical College and by the Institutional Review Board of National Cancer Center.

Tissue microarray construction

We constructed TMA blocks as previously described [16]. Briefly, double tissue cores with a diameter of 2 mm were obtained from each donor block, and these core specimens were transferred to a recipient block using a Tissue Microarrayer (Beecher Instruments, Silver Spring, MD, USA). One TMA block contained a maximum of 26 tumor samples, and 13 TMA sets were used in this study.

Immunohistochemistry

Immunohistochemistry was performed on TMA sections of 220 patients. The antibodies used were mouse monoclonal anti-human NS (clone BL2858; Bethyl Laboratories, Inc., Montgomery, TX, USA) and mouse monoclonal anti-human p53 (clone DO-7; Dako, Carpinteria, CA, USA). Formalin-fixed paraffin-embedded specimens on the TMA were cut into 4 μm-thick sections. The tissue sections were deparaffinized twice in xylene for 10 min and rehydrated through graded ethanol (99%, 90%, 80%, and 70%) to water. Antigens were retrieved by microwave heating for 30 min in 10 mM sodium citrate (pH 6.0) for NS and by autoclaving for 15 min in 10 mM Tris–HCl (pH 9.0) for p53. To block endogenous peroxidase activity, the sections were treated with 100% methanol containing 3% hydrogen peroxide for 5 min. Non-specific binding was blocked by incubation in 2% normal swine serum (Dako) in phosphate-buffered saline. The slides were incubated with primary antibodies at 4°C overnight and then reacted with a dextran polymer reagent combined with secondary antibodies and peroxidase (Envision Plus; Dako) for 30 min at room temperature. Specific antigen–antibody reactions were visualized with 0.2% diaminobenzidine tetrahydrochloride and hydrogen peroxide. Counterstaining was performed using Mayer's hematoxylin. A separate assay was run using a case of esophageal carcinoma as a positive control for NS [17]. Reactions without the primary antibodies were used as negative controls.

Table 1 Correlation between nucleostemin expression and clinicopathological variables in surgically resected breast cancers

Variable	Number of cases (%)			
		Nucleostemin expression		
	Total	Positive	Negative	P-value
	(n = 220)	(n = 142)	(n = 78)	
Age				
Median (range)		52 (30 ~ 82 y)		
≦52	109	71 (65)	38	0.89
>52	111	71 (64)	40	
Tumor size				
<5.0 cm	174	108 (62)	66	0.21
≧5.0 cm	42	31 (74)	11	
Unknown	4	4(100)	0	
Lymph node metastasis				
Negative	115	70 (61)	45	0.39
Positive	101	68 (67)	33	
Unknown	4	4 (100)	0	
Distant metastasis				
Negative	209	134 (64)	75	0.72
Positive	8	6 (75)	2	
Unknown	3	2 (67)	1	
Stage				
I or II	179	111 (61)	68	0.13
III or IV	37	28 (76)	9	
Unknown	4	3 (75)	1	
Nuclear grade				
1, 2	137	86 (63)	51	0.48
3	83	56 (67)	27	
ER status				
Negative	88	50 (57)	38	0.050
Positive	132	92 (70)	40	
PgR status				
Negative	96	57 (59)	39	0.16
Positive	124	85 (69)	39	
HR (ER/PgR) status				
Negative	66	40 (61)	26	0.42
Positive	154	102 (66)	52	
HER2 status				
Negative	190	117 (62)	73	0.02
Positive	30	25 (83)	5	
p53 status				
Negative	143	85 (59)	58	0.03
Positive	77	57 (74)	20	
Histological type				
Ductal	191	125 (65)	66	0.38
Lobular	10	5 (50)	5	
Mucinous	6	6 (100)	0	
Tubular	5	1 (20)	4	
Medullary	3	2 (67)	1	
Other	5	3 (60)	2	

Abbreviation: ER Estrogen receptor, *PgR* Progesterone receptor, *HR* Hormone receptor.

NS and p53 expression was assessed according to the proportion of nuclear staining area. Specimens with 10% or more immunoreactive tumor cells were considered positive, and those with less than 10% were considered negative. Immunohistochemistry results were independently evaluated by two observers (T.K. and H.T.), and cases with discrepant grades were re-evaluated by discussion until consensus was achieved.

ER, PgR, and HER2 had already been immunohistochemically re-assessed on new sections in our previous study [16] by using mouse monoclonal anti-human ER (clone 1D5, Dako), mouse anti-human PgR (clone PgR636, DAKO), and rabbit polyclonal anti-HER2 antibody (HercepTest kit, Dako) according to the methods recommended by the manufacturer. ER and PgR were considered positive if the nuclear staining was observed in 10% or more of tumor cells. Samples were considered hormone receptor positive if they were ER and/or PgR positive and hormone receptor negative if they were ER and PgR negative. HER2 results were considered positive if the IHC score was "3+" or gene amplification was detected by FISH according to the 2007 ASCO/CAP guideline [18].

Statistical analysis

Comparisons between groups were evaluated using chi-squared test or Fisher's exact test. Disease-free survival (DFS) curves of patients were drawn using the Kaplan-Meier method and compared using the log-rank test. Cox multivariate proportional hazards models were used to explore the association of variables with DFS. For all tests, $P < 0.05$ was considered to be statistically significant. All analyses were performed using the software JMP 6.0 for Windows (SAS Institute Inc., Cary, NC, USA).

Results

Clinicopathological and prognostic implications of NS expression for the entire patient cohort

Initially, the expression levels of NS were classified as negative (0%), weak (1% to <10%), moderate (10% to <30%), or strong (30% or more). The number of cases categorized